SUPPLEMENTAL INFORMATION

Supplemental Information includes additional experimental procedures as well as six figures that directly support main figures presented in the paper.

SUPPLEMENTAL EXPERIMENTAL PROCEDURES

Fluoro-Gold Experiments

Immediately following paraformaldehyde perfusions, brains were removed, post-fixed overnight in 4% paraformaldehyde and sectioned in 100 µm coronal slices on a VT-1200 vibratome (Leica, Nussloch, Germany). Sections were permeabilized for 15 minutes in PBS with 0.2% Triton-X 100 (PBST), washed three times, five minutes each, in PBS, blocked 1 hour in 3% normal goat serum in PBS, washed again three times, five minutes each, in PBS and incubated overnight in rabbit anti-Fluoro-Gold (AB153; Millipore; Billerica, MA) diluted 1 to 10,000 in PBST with 1% normal goat serum. The next day, sections were washed five times, five minutes each, in PBS, incubated 1 hour in Cy3-conjugated anti-rabbit (Jackson Immunolabs) diluted 1 to 500 in PBS, washed three times, five minutes each, in PBS and mounted on glass slides. Following brief air drying, sections were mounted using Vectashield with DAPI (Vector Labs).

Slides were scanned on a confocal microscope (Olympus) with a 10X objective, isolating a single Z-plane. One section was chosen in each brain region from each mouse that represented the maximal labeling for each brain region. Cells in the ipsilateral hemisphere were manually counted in each of these sections by identifying the number of discrete cell bodies visible with signal clearly above background. Background for each brain region was determined by examining tissue from a control mouse that did not receive an injection of Fluoro-Gold, but was prepared and immunostained in parallel with the other mice. Total fluorescence was calculated in each brain slice in the specific areas of the prefrontal cortex, basolateral amygdala, and ventral hippocampus where NAc-projecting cells were located.

Electrophysiology

Brains were sectioned around both the injection site and the NAc in 200 µm thick coronal sections on a VT-1200 vibratome (Leica). The artificial cerebrospinal fluid (ACSF) used to both perfuse the animals and slice the brains was modified to contain (in mM): 75 sucrose, 87 NaCl, 2.5 KCL, 1.25 NaH_2PO_4, 7 $MgCl_2$, 0.5 $CaCl_2$, 26 $NaHCO_3$, 11 glucose and 3 sodium ascorbate. Slices were placed in a holding chamber filled with 32°C ASCF saturated with 95% O_2 and 5% CO_2 containing (in mM): 125 NaCl, 2.5 KCl, 1.25 NaH2PO4, 1 MgCl2, 2.4 CaCl2, 26 NaHCO3, 11 glucose and 1 sodium ascorbate. The ACSF used in the recording chamber was the same except for the exclusion of sodium ascorbate and, to block inhibitory transmission, the addition of picrotoxin (100 µM). Electrodes (3-5 MΩ) were backfilled with an internal solution containing (in mM): 117 cesium methanesulfonate, 20 HEPES, 0.4 EGTA, 2.8 NaCl, 5 TEA-Cl, 4 Mg-ATP and 0.4 Na-GTP (280-285 mOsm). Cells were visualized on an upright microscope using infrared differential interference contrast video microscopy. Whole-cell voltage-clamp recordings were made using a MultiClamp 700B amplifier (2 kHz low-pass Bessel filter and 10 kHz digitization) with pClamp 10.3 software (Molecular Devices). Medium spiny neurons in the medial NAc shell were identified by morphology, membrane resistance, and hyperpolarized resting membrane potential. Series resistance (10-25 MΩ) was monitored with a 5 mV hyperpolarizing pulse (50 ms) given every 20 s, and only recordings that remained stable over the period of data collection were used. The current-voltage relationship of excitatory currents was obtained with optical stimulation using an internal solution that contained 3 mM QX-314. AMPAR current-voltage relationships were examined with 50 uM AP5 in the superfused ACSF and 100 uM spermine in the internal solution. NMDAR current-voltage relationships were collected with 10 uM CNQX in the superfused ACSF. All drugs were obtained from either Sigma or Tocris Bioscience.

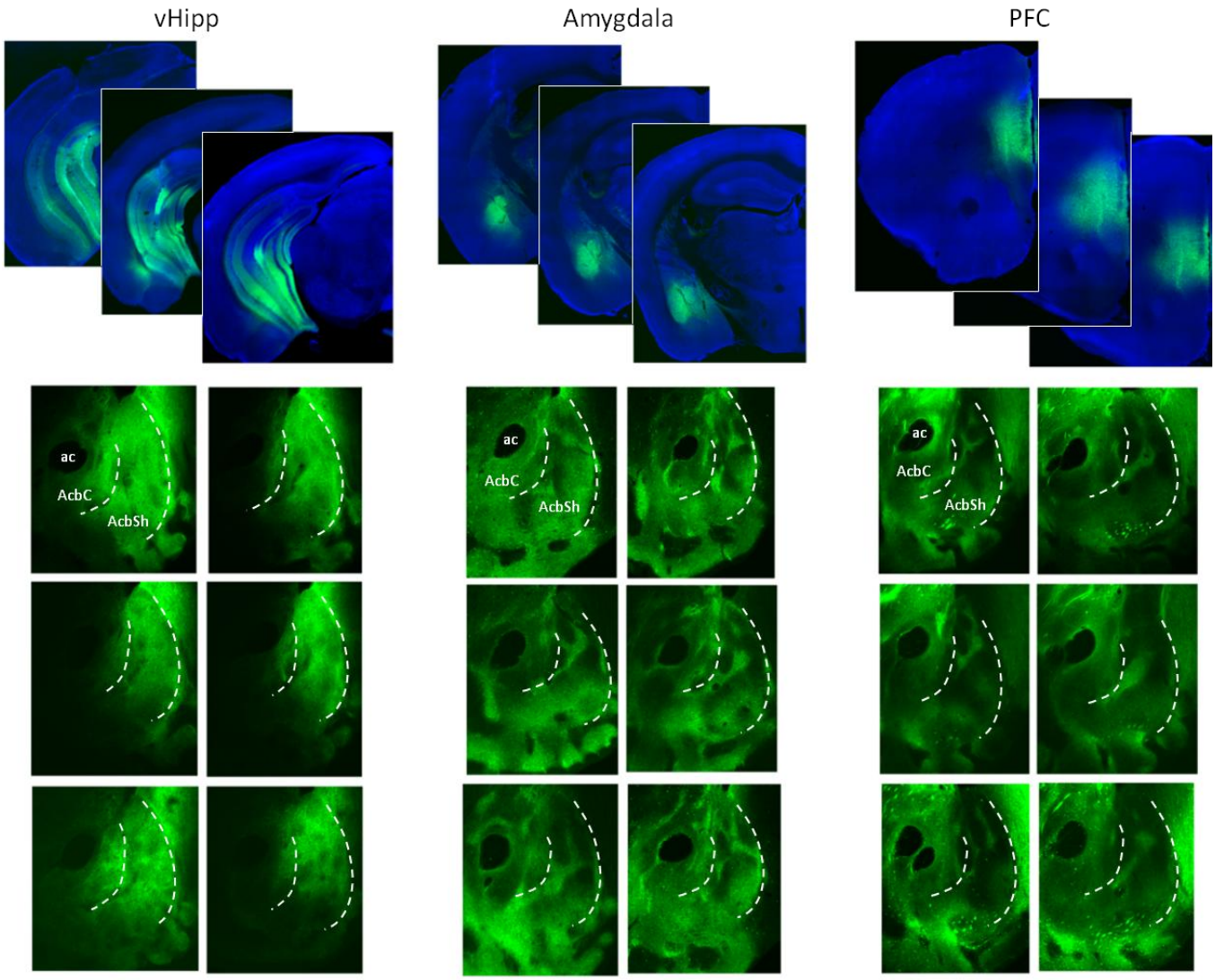

Figure S1, related to Figure 1. vHipp Input to the NAc is Uniquely Concentrated in the Medial Shell
Representative coronal brain slices showing expression of EYFP (green) after virus injection into the vHipp, basolateral amygdala, or prefrontal cortex. The top row shows images from the sites of virus injection. The bottom rows show images of EYFP-expressing afferents to the NAc. Notice the relatively selective innervation of the medial NAc shell from the vHipp axons.

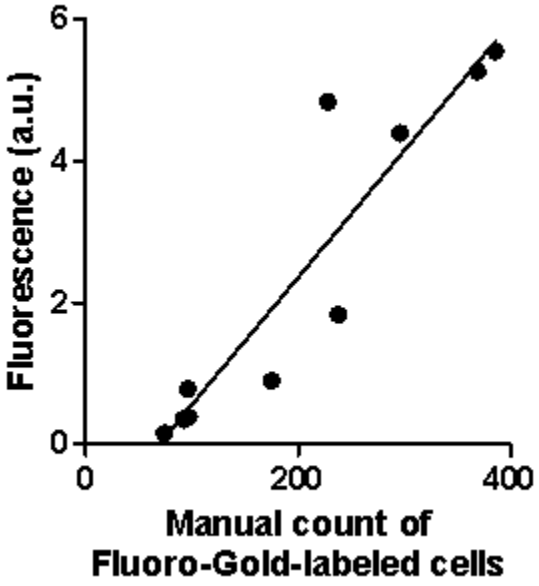

Figure S2, related to Figure 2. Fluorescence Intensity Correlates with Manual Cell Counts of Immunolabeled Cells

Immunolabeled-Fluoro-Gold fluorescence significantly correlated with manual cell counts of Fluoro-Gold labeled cells (n = 10; R^2 = 0.86, P < 0.01). The x-axis represents manual counts of the number of Fluoro-Gold-positive cell bodies within different brain regions (vHipp, amygdala, prefrontal cortex) following Fluoro-Gold injections into the NAc shell. The y-axis represents total fluorescence signal in each brain region. Total fluorescence was calculated within regions of interest (ROI) by multiplying mean fluorescence by the surface area of the ROI. The ROI for each slice was defined by the subregion of tissue containing Fluoro-gold positive cell bodies, and was manually traced. Mean fluorescence for each slice was determined in Adobe Photoshop by measuring the average pixel intensity in the red channel, with background subtracted – defined by average red channel pixel intensity of a region of grey matter without anti-Fluoro-Gold fluorescence.

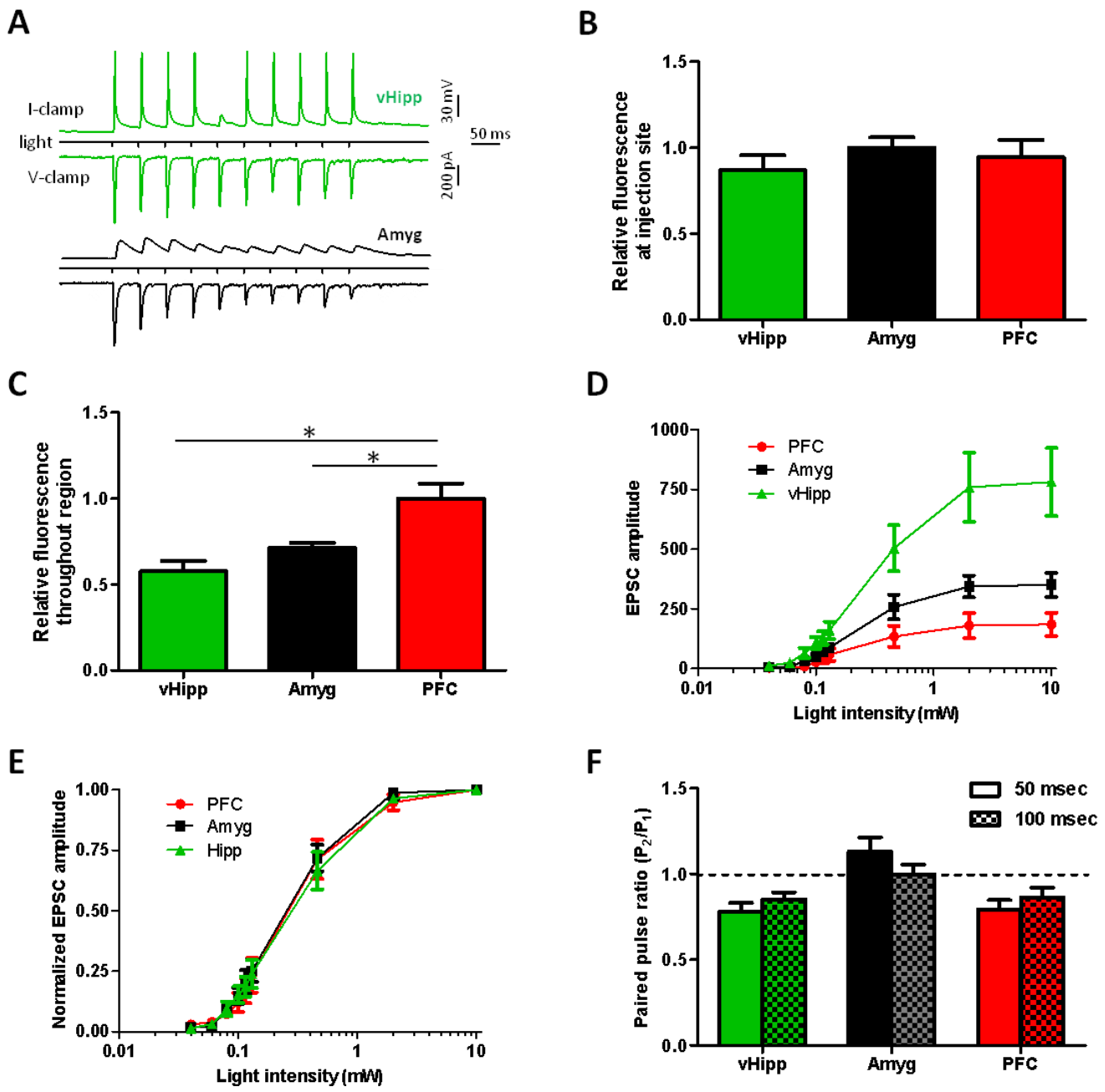

Figure S3, related to Figure 3. vHipp Input to the Medial NAc Shell is Uniquely Effective in Driving Postsynaptic Spiking

(A) Representative current- and voltage-clamp recordings from medium spiny neurons in the medial NAc shell during optical stimulation (20 Hz) of ChR2-postive axons coming from the vHipp (top) and basolateral amygdala (bottom). Physiological recording solutions were used. (B) The intensity of the fluorescent signal at the different injection sites, relatively to the brightest average signal, show viral injections and ChR2 expression is similar between injection sites (n = 5, 4, and 5 for the vHipp, amygdala, and prefrontal cortex injections, respectively; one-way ANOVA, $F_{(2,11)} = 0.5$, $P > 0.05$). (C) The average fluorescent intensity of each region, calculated across brain slices throughout areas where NAc-shell projection neurons were located, suggests a relatively larger proportion of NAc-projecting neurons were virally-infected in the prefrontal cortex (n = 5, 4, and

5 for the vHipp, basolateral amygdala, and prefrontal cortex injections, respectively; one-way ANOVA, $F_{(2,11)}$ = 10.7, P < 0.01; *post hoc* test of prefrontal cortex versus vHipp and amygdala, p < 0.05). (D) Summary of optically-evoked EPSC amplitudes measured at different light intensities in different afferent pathways to NAc shell medium spiny neurons (*n* = 7, 6 and 7 for the vHipp, amygdala and prefrontal cortex inputs, respectively; repeated measures ANOVA, significant interaction, $F_{(16,136)}$ = 7.9, P < 0.01). (E) Normalized input-output curves from the data presented in (D) suggest each input pathway has comparable amounts of functional ChR2 protein (repeated measures ANOVA, pathway effect, $F_{(2,136)}$ = 0.1, P > 0.05). (F) Paired pulse ratios (P_2/P_1) show that only amygdala afferents exhibit paired pulse facilitation, suggesting a lower presynaptic vesicle release probability in this pathway (*n* = 52, 39 and 37 for both of the vHipp, amygdala and prefrontal cortex measurements, respectively; two-way ANOVA, location main effect, $F_{(2,230)}$ = 10.8, P < 0.05).

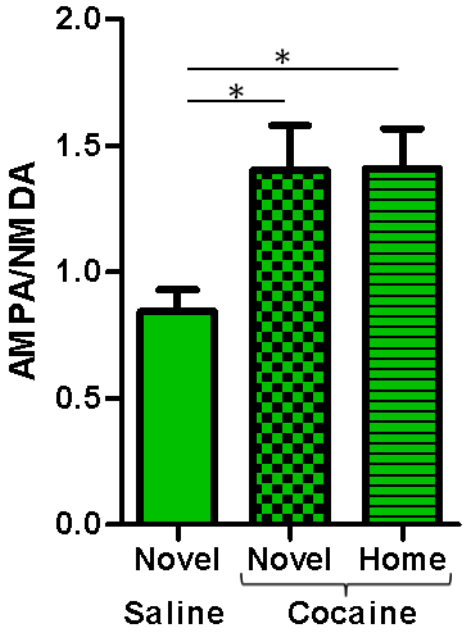

Figure S4, related to Figure 5. vHipp Afferents to the NAc Shell are Potentiated Following Cocaine Injections
Summary of AMPA/NMDA receptor response ratios show vHipp input is selectively potentiated following repeated cocaine injections, regardless of where the cocaine was administered (*n* = 10, 9, and 9 for the saline, novel cocaine, and home cocaine, respectively; one-way ANOVA, $F_{(2,25)}$ = 5.5, P < 0.05; *post hoc* test of cocaine versus saline treatments, p < 0.01).

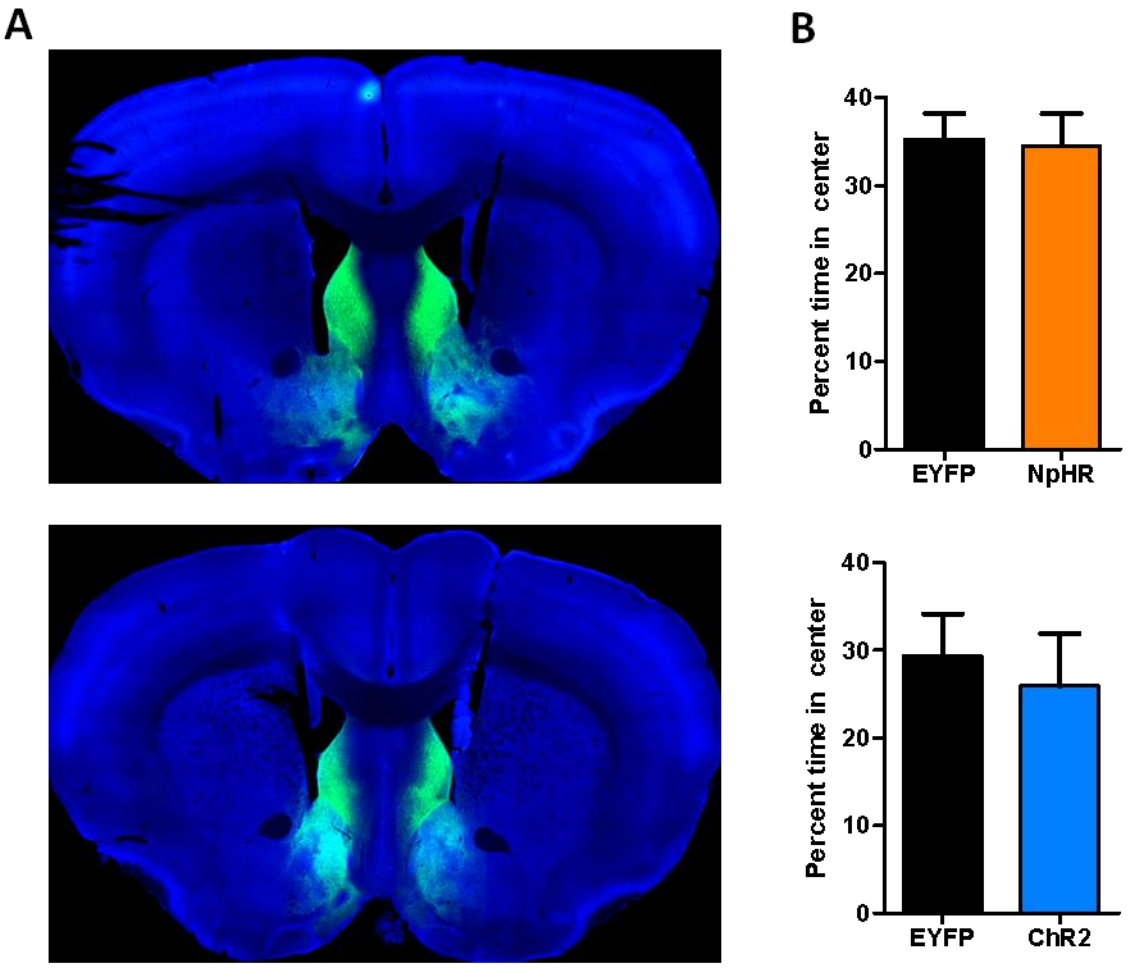

Figure S5, related to Figure 6. Activity of vHipp Axons in the NAc Does Not Alter Anxiety-Related Behavior
(A) Representative coronal brain slices showing tracts of implanted optical fibers and expression of NpHR-EYFP (green; top) or ChR2-EYFP (bottom) in the NAc after virus injection into the vHipp. Images are counterstained with the nuclear dye DAPI (blue). (B) Summary of the proportion of time mice spent exploring the center of an open field chamber, a measure of anxiety-related behavior (n = 4 for each group; EYFP vs NpHR, t_6 = 0.2, P > 0.05; EYFP vs ChR2, t_6 = 0.2, P > 0.05).

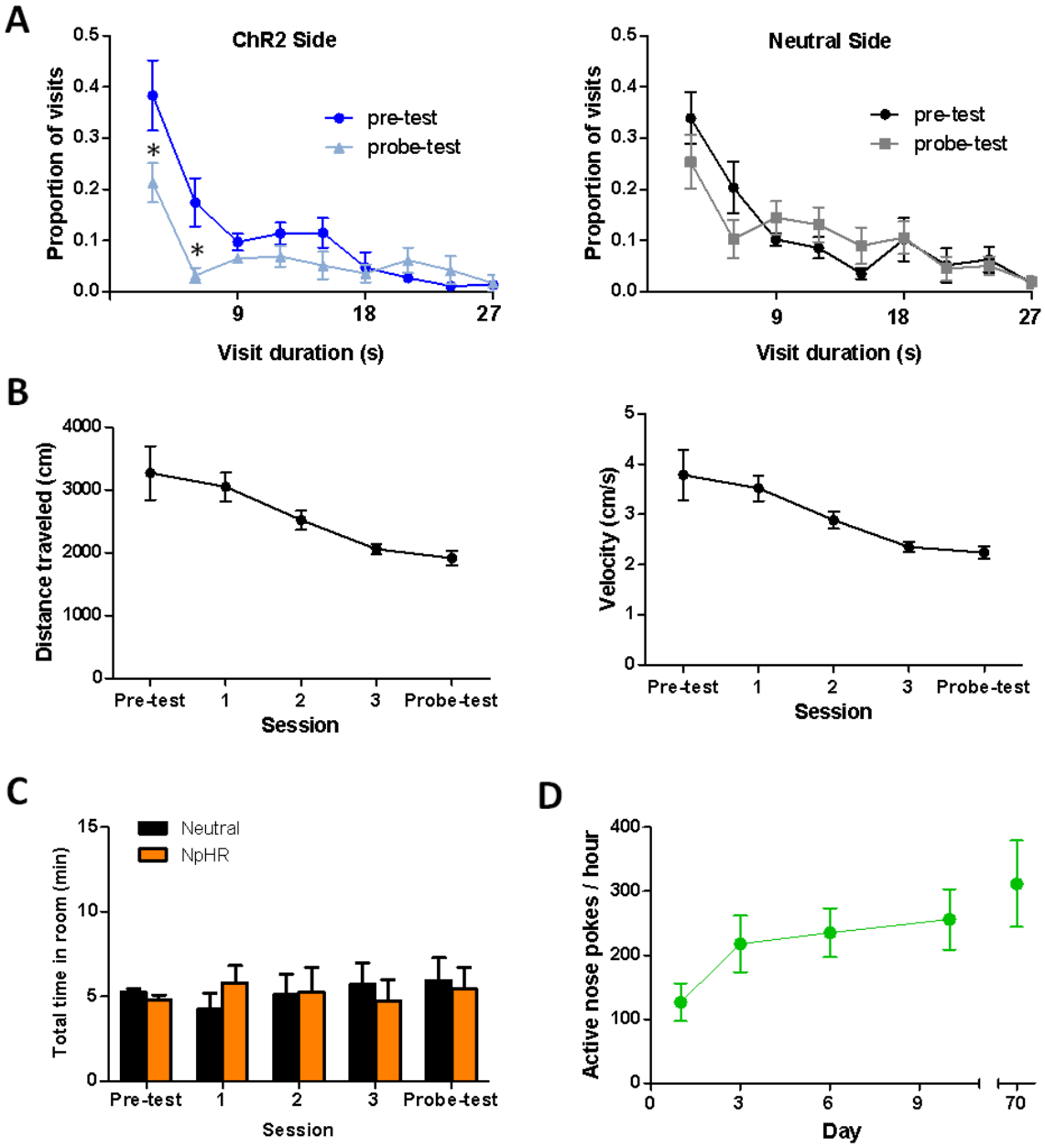

Figure S6, related to Figure 7. Optical Activation of vHipp Axons in the NAc Induces a Place Preference by Reducing the Probability Mice Will Exit from the ChR2-Paired Side of the Chamber

(A) Plotting the distributions of visit durations for each side of the chamber on pre- and probe-test days shows an exponential distribution similar to that observed in classical conditioned place preference experiments. On the probe test day versus the pre-test day, mice made fewer quick visits to the ChR2-paired side (n = 6; repeated measures ANOVA on ChR2-paired side, significant interaction, $F_{(8,45)} = 2.7$, $P < 0.05$; *post hoc* test for visit durations lasting either 3 or 6 seconds or less, $p < 0.05$). (B) Summary of locomotor behavior in a place preference chamber where one side is paired with the optical stimulation of vHipp axons in the NAc shell. (C) Summary of time spent in different sides of a real-time place preference chamber over five consecutive days (n = 12; repeated measures ANOVA, $P < 0.05$). During the three test sessions, vHipp axons in the NAc were optically inhibited whenever mice entered and remained in the NpHR-paired side of the chamber. (D) Average number of active nose pokes made by mice to obtain optical activation of vHipp axons in the NAc in sessions spanning 70 days.